ELSEVIER

Biophysical Chemistry 119 (2006) 127 – 136

Biophysical Chemistry

http://www.elsevier.com/locate/biophyschem

Ab initio studies on the tri- and diphosphate fragments of adenosine triphosphate

Priti Hansia, Nandini Guruprasad, Saraswathi Vishveshwara *

Molecular Biophysics Unit, Indian Institute of Science, Bangalore, 560012, India

Received 27 May 2005; received in revised form 26 July 2005; accepted 28 July 2005
Available online 26 August 2005

Abstract

Pyrophosphate prototypes such as methyl triphosphate and methyl diphosphate molecules in their different protonation states have been investigated at high levels of quantum chemical calculations. The optimized geometries, the thermochemistry of the hydrolysis and the molecular orbitals contributing to the high energy of these compounds have been analyzed. These investigations provide insights into the "high energy" character of ATP molecule. Further, the dependence of vibrational frequencies on the number of phosphate groups and the charged states has also been presented. These results can aid the interpretation of spectra obtained by experiments on complexes containing pyrophosphate prototypes.

Keywords: "High energy" of pyrophosphates; Hydrolysis of P–O–P linkage; Delocalized molecular orbitals; Frequencies of polyphosphates

1. Introduction

In living cells, Adenosine triphosphate (ATP) is considered as the universal energy-transfer molecule. The most common medium of energy exchange in the cells is phosphate compounds. The exothermic process of the hydrolysis of these compounds is coupled to virtually all the biosynthetic reactions. The pyrophosphate (P–O–P) linkage plays a role of supreme importance in the chemistry of these phosphorus compounds. Molecules incorporating this linkage are involved in a vast variety of chemical environments and applications, from inorganic to biological systems [1,2]. The P–O–P linkage is not found in nature except as produced by living organisms because of its high susceptibility to hydrolysis. The chemical energy derived from the hydrolysis of this P–O–P linkage of adenine and guanine di- and triphosphates (i.e., ADP, ATP, GDP and GTP) is used by the cells to carry out different biological functions. Although the chemistry of pyrophosphates and ATP is quite different, the pyrophosphate linkage is a prototype for understanding the chemistry of ATP and a careful study of the species involving this linkage may be able to provide important information about ATP as well. For this reason, model species comprising the pyrophosphate linkage have been the subject of intensive theoretical studies for many years and crystal structures of molecules containing pyrophosphates have also been determined [3].

Biologically important compounds with large negative free energies of hydrolysis at physiological pH have been described as "high energy" compounds, phosphate compounds with pyrophosphate linkage being one of them. Although the idea of "high energy" phosphates has been current for more than 70 years [4,5] and has proved indispensable for an understanding of energy storage and energy transfer in biological systems, there has not yet appeared any clear explanation as to why certain phosphate compounds contain more energy than do ordinary ester phosphates. For a long time the energetic capabilities of these "high energy" phosphate compounds were originally thought to be due to purely intramolecular effects ranging from simple electrostatic repulsions and electron distribu-

* Corresponding author. Tel.: +91 80 2293 2611; fax: +91 80 2360 0535.
E-mail address: sv@mbu.iisc.ernet.in (S. Vishveshwara).

0301-4622/$ - see front matter © 2005 Elsevier B.V. All rights reserved.
doi:10.1016/j.bpc.2005.07.011

tions along the P–O–P backbone to more complex 'opposing resonance' effects [6–12]. Considering the importance of hydrolysis of these phosphate compounds, quantum mechanical studies have also been carried out to assist in understanding these species and their reactions [13–17]. Many of the investigations have been carried out at the Hartree–Fock level. However the electron correlation plays a major role imparting unusual properties to this molecule and hence it is important to investigate these systems at the levels which include rigorous correlation energy evaluation.

In the last few years there have been lots of reports on quantum chemical studies on the energetics of the origin of hydrolyzing a pyrophosphate linkage. Colvin et al. [16] performed large basis set ab initio calculations of the reaction energy for pyrophosphate hydrolysis. These calculations were performed using second order Möller–Plesset perturbation theory (MP2) at the Hartee–Fock/6-311+G** optimized geometries. They have also predicted the aqueous phase hydration energy using several methods based on a dielectric continuum model of the aqueous solvent. Recently, the energetics of the rotation of the pyrophosphate linkage has also been investigated by the use of ab initio calculations by Hwang et al. [17]. They have explored the potential energy surface of three pyrophosphate prototypes using HF/6-31G* basis set. Experimental and theoretical studies on vibrational frequencies of molecules containing the pyrophosphate linkage (or phosphate group) have also been reported [18,19]. Time resolved Fourier transform infrared (FTIR) difference spectroscopy has much been used to study these kinds of molecules [19].

Several studies [8,11,13–16] have indicated that the electrostatic effects play an important role both in the molecular structure and thermochemistry of the hydrolysis of pyrophosphates. There is no doubt that this is true and these factors are strongly influenced by environmental factors such as the counter ion, pH and the concentration of solute and cation, as evidenced by experiments. An in-depth study of these factors at ab initio level is difficult since the simulation of environment is complex. However, we believe that the inherent nature of the pyrophosphate should also be a significant reason for the "high energy" character of the pyrophosphate. There are two aspects to the "high energy" property of the pyrophosphate molecules, which are (1) the process of hydrolysis and (2) storage and release of energy by the molecules with pyrophosphate groups. Several investigations have focused on the process of hydrolysis. Our present study also elucidates this process at MP2 level of theory, by investigating the thermochemistry and vibrational frequencies of different ionic species of pyrophosphates. The specific prototype systems investigated are: methyl triphosphate (MTP: $CH_4P_3O_{10}^{-3}$, $CH_5P_3O_{10}^{-2}$, $CH_6P_3O_{10}^{-1}$), methyl diphosphate (MDP: $CH_4P_2O_7^{-2}$, $CH_5P_2O_7^{-1}$) and methyl monophosphate (MMP: $CH_4PO_4^{-1}$), and their structures are shown in Fig. 1. The molecular orbitals in all these systems are analyzed in detail, which gives some insight into the inherent capacity of the pyrophosphates to posses "high energy" character.

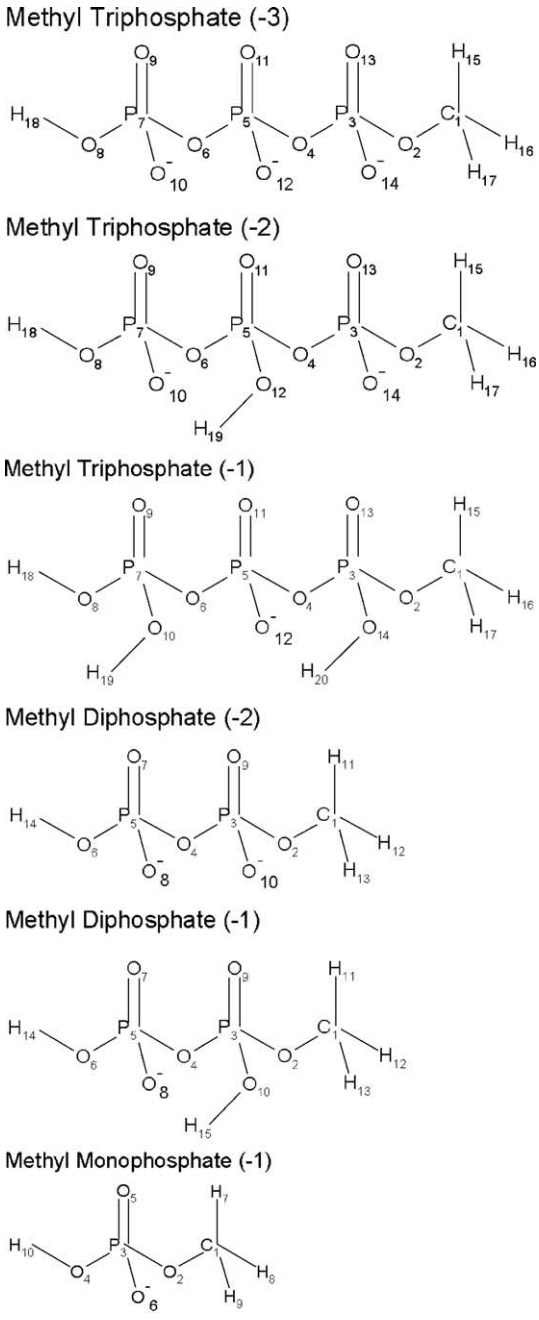

Fig. 1. Schematic representation of the six model compounds under investigation.

2. Methods

The initial geometries of all the molecules in Fig. 1 were generated using the bond length and bond angle information either from the crystal structure of the disodium complex of ATP [3] or from standard parame-

Table 1
Optimized bond lengths (Å) of molecules shown in Fig. 1

Theory/basis-set	System	O_2-P_3	P_3-O_4	O_4-P_5	P_5-O_6	O_6-P_7	P_7-O_8
MP2/6-31G*	MTP(−3)	1.6930	1.6576	1.6761	1.6561	1.6938	1.6535
	MTP(−2)	1.6561	1.6889	1.6204	1.6058	1.7279	1.6131
	MTP(−1)	1.6261	1.6228	1.6525	1.6658	1.6437	1.6144
	MDP(−2)	1.7090	1.6488	1.6560	1.7031		
	MDP(−1)	1.6376	1.5993	1.7156	1.6475		
	MMP(−1)	1.6878	1.6674				
MP2/6-31++G**	MTP(−3)	1.6910	1.6545	1.6703	1.6585	1.6867	1.6576
	MTP(−2)	1.6851	1.6935	1.6088	1.6259	1.6968	1.6325
	MTP(−1)	1.6256	1.6220	1.6520	1.6705	1.6407	1.6168
	MDP(−2)	1.7055	1.6422	1.6471	1.7042		
	MDP(−1)	1.6358	1.6010	1.7157	1.6501		
	MMP(−1)	1.6869	1.6682				

ters. Potential energy scans on the dihedral angles O–P–O–P and P–O–P–O were carried out at HF level using 6-31G* basis set. The lowest energy conformation in the dihedral angle space was considered for complete optimization. The fully optimized geometries of methyl triphosphate (MTP), methyl diphosphate (MDP) and methyl monophosphate (MMP) were obtained by the analytical gradient methods using the basis sets 6-31G* [20] and 6-31++G** [21]. The calculations were performed using Gaussian98 and Gaussian03 [22] programs at the levels of Hartree–Fock (HF), Density Functional Theory (B3LYP) [23] and second order Möller–Plesset (MP2) [24] theories. The default "fine" integration grid (corresponding to Int=FineGrid) and the default convergence criteria (Maximum Force threshold=0.000450, RMS Force threshold=0.000300, Maximum Displacement threshold=0.001800 and RMS Displacement threshold=0.001200) were used for DFT calculations. MP2 optimized geometrical details are presented in the main paper and a comparison with the values obtained from HF and DFT calculations (given in the supporting information) is made in the text. Furthermore, the optimized geometries were used to carry out calculations on vibrational frequencies on the different systems with HF, DFT and MP2 levels of theory. The frequency modes were identified from Molden [25].

3. Results and discussion

3.1. Geometry optimization

As mentioned above, the potential energy scans as functions of dihedral angles O–P–O–P and P–O–P–O were carried out on MTP and MDP systems presented in Fig. 1. All-trans conformations were found to be the lowest energy conformations in these systems and these conformations were used as the starting point for complete geometry optimization at HF, DFT and MP2 levels. The total optimized energies and zero-point vibrational energies of various charged forms of MTP, MDP and MMP are given in Table SI for 6-31++G** basis set. The energy differences between various phosphate compounds given in Fig. 1 show a consistent pattern at all the levels of calculations.

The optimized geometries of all the systems have been analyzed in terms of the bond lengths, bond angles and dihedral angles. The MTP systems have six P–O bonds (Fig. 1). The optimized lengths of these bonds along with the equivalent P–O bonds in MDP and MMP obtained from 6-31G* and 6-31++G** basis sets at MP2 level are presented in Table 1. (The corresponding values obtained at HF and DFT levels are given in Table SII).

The bond distances in general are shorter as evaluated at HF level (both basis sets, 6-31G* and 6-31++G**), in com-

Table 2
Optimized bond angles (°) of molecules shown in Fig. 1

Theory/basis-set	System	$C_1-O_2-P_3$	$O_2-P_3-O_4$	$P_3-O_4-P_5$	$O_4-P_5-O_6$	$P_5-O_6-P_7$	$O_6-P_7-O_8$
MP2/6-31G*	MTP(−3)	114.4	100.5	133.5	95.6	127.4	99.6
	MTP(−2)	116.0	100.7	132.8	107.1	127.3	99.0
	MTP(−1)	115.4	98.7	126.1	97.5	118.6	102.2
	MDP(−2)	111.3	91.7	133.8	92.2		
	MDP(−1)	114.9	100.4	126.6	100.1		
	MMP(−1)	112.4	96.0				
MP2/6-31++G**	MTP(−3)	116.0	101.3	136.4	96.1	129.0	100.1
	MTP(−2)	118.6	98.8	135.0	105.2	131.2	100.6
	MTP(−1)	116.5	98.8	126.0	97.4	118.7	102.5
	MDP(−2)	112.7	92.2	139.3	92.7		
	MDP(−1)	116.2	100.3	126.1	106.3		
	MMP(−1)	114.1	96.6				

Table 3
Optimized dihedral angles (°) of molecules shown in Fig. 1

Theory/basis-set	System	$C_1-O_2-P_3-O_4$	$O_2-P_3-O_4-P_5$	$P_3-O_4-P_5-O_6$	$O_4-P_5-O_6-P_7$	$P_5-O_6-P_7-O_8$
MP2/6-31G*	MTP(−3)	77.3	−96.9	167.9	139.9	−48.3
	MTP(−2)	67.0	41.0	39.8	78.9	−111.8
	MTP(−1)	178.2	−73.6	−120.6	−177.8	−54.3
	MDP−2)	180.0	180.0	−180.0		
	MDP(−1)	177.4	−74.5	92.3		
	MMP(−1)	173.6				
MP2/6-31++G**	MTP(−3)	77.9	−89.9	160.0	137.1	−44.0
	MTP(−2)	−111.2	25.4	−78.8	100.6	−99.7
	MTP(−1)	−178.1	−72.4	−122.7	−177.9	−54.9
	MDP(−2)	179.9	179.9	−180.0		
	MDP(−1)	179.9	−72.0	89.9		
	MMP(−1)	166.9				

parison with DFT or MP2 levels of calculations. The P–O bond length ranges are (1.57–1.7 Å), (1.59–1.74 Å) and (1.60–1.73 Å) as obtained at HF, DFT and MP2 levels respectively. However, all the methods in general have predicted a consistent trend for a given molecule. For instance, the shortest P–O distance for MTP(−3) system is predicted to be for P_3-O_4 by most of the levels of calculations (with the exception of DFT/6-31G* and MP2/6-31G*) and the longest distance is obtained either for O_2-P_3 or O_6-P_7 for all the systems by all the levels of calculations. It is interesting to see that the length of the P–O bond depends not only on the number of phosphate units in the molecule, but also on the protonation state. The optimized bond angles obtained at MP2 level for all the systems have been tabulated in Table 2 and the corresponding values obtained at HF and DFT levels are given in Table SIII. In general, the angles at the phosphorous atoms are smaller (92°–107°) and the angles at the oxygen atoms are larger (119°–149°, considering only P–O–P angle) than the tetrahedral value. A large variation of the POP angle at the oxygen atoms can be seen from these tables. The values depend on the number of phosphate units and the protonation states as observed in the case of P–O bond lengths.

The optimized torsion angles for all the systems under investigation have given insightful information about the overall geometry of the systems. Table 3 gives the details of these torsion angles at MP2 level whereas Table SIV gives the details at HF and DFT levels. It is interesting to note that the optimized geometry is no longer all-trans in many cases. It is known that all-trans geometry is not the minimum energy conformation in systems containing -(O–C–O)- or -(O–P–O)- groups due to anomeric effect [26,27]. This was explained to be due to the factors such as delocalization of electronic orbitals, dipole interactions and steric effects [28]. It is impressive to observe a similar trend even in the systems as complex as MTP. MDP(−2) is the only system under investigation to yield a (t,t) optimized conformation for the rotation around the bonds P_3-O_4 and O_4-P_5. This conformation for MDP(−2) is observed by all the levels of calculations with the exception of DFT/6-31++G**. In all other systems, a variety of torsion angle combinations are adopted. Once again, the optimized conformations have been found to be dependent on the number of phosphate groups and the protonation state of the molecule.

The optimized geometries of the MTP and MDP systems at MP2/6-31++G** level are presented in Fig. 2. The protonation state affects the type and the number of intramolecular hydrogen bond, which has an influence on the overall geometry of the molecules. MTP(−3) system shows only one intramolecular H-bond, whereas MTP(−2) and MTP(−1) systems show two and three intramolecular H-bonds, respectively. Similarly, MDP(−1) adopts a conformation with one intramolecular hydrogen bond. The donor–acceptor (O...O) bond lengths in all these systems range from 2.54 Å to 2.83 Å and O–H..O bond angles range from

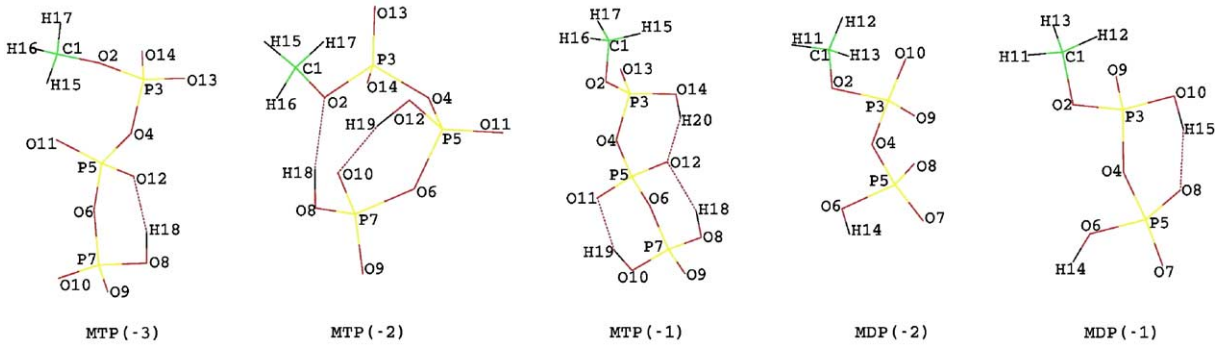

Fig. 2. MP2/6-31++G** optimized geometries of MTP(−3), MTP(−2), MTP(−1), MDP(−2) and MDP(−1).

Table 4
Energy of hydrolysis including ZPVE (in Kcal/Mol) in gas phase of reactions R1–R5 at 6-31++G** basis set

Reaction	HF	DFT/B3LYP	MP2
R1	−96.41	−168.36	−86.03
R2	−48.54	−48.77	−48.49
R3	13.74	14.11	12.60
R4	−77.19	−62.39	−77.43
R5	21.70	22.06	20.41

152° to 163° at MP2 level. Very similar results are obtained at DFT as well as at HF levels. However, HF level in general predicts a longer O...O bond length.

3.2. Thermochemistry of the gas phase hydrolysis

We have analyzed the thermochemical data for the following reactions.

$$CH_4P_3O_{10}^{-3} + H_2O \rightarrow CH_4P_2O_7^{-2} + H_2PO_4^- \quad (R1)$$

$$CH_5P_3O_{10}^{-2} + H_2O \rightarrow CH\pm_5P_2O_7^{-1} + H_2PO_4^- \quad (R2)$$

$$CH_6P_3O_{10}^{-1} + H_2O \rightarrow CH_5P_2O_7^{-1} + H_3PO_4 \quad (R3)$$

$$CH_4P_2O_7^{-2} + H_2O \rightarrow CH_4PO_4^{-1} + H_2PO_4^- \quad (R4)$$

$$CH_4P_2O_7^{-1} + H_2O \rightarrow CH_4PO_4^{-1} + H_3PO_4 \quad (R5)$$

The hydrolysis energies corresponding to these reactions at different levels of calculations have been tabulated in Table 4. These hydrolysis energies obtained from different levels of theory are very much comparable with the exception of the reaction R1 at DFT level. As can be seen from Table 4, the above reactions have strong electrostatic effects and result is qualitatively similar to that of the previous study carried out by Ma et al. [15] on MDP. Hydrolysis of reactions R1, R2 and R4 is strongly exothermic, whereas that of reactions R3 and R5 is endothermic. Also, the absolute value of the hydrolysis energy is dependent on the charge state of the molecule. R1 has more negative hydrolysis energy than R2. These results point out that electrostatic effects are very predominant in these reactions. Reactions R3 and R5 are endothermic because the molecules involving these reactions are monoanions and electrostatic attraction rather than electrostatic repulsion should significantly predominate these reactions. Similar reasons can be given to explain the exothermicity of reactions R1, R2 and R5. Electrostatic repulsions clearly are responsible for this exothermicity, which has been pointed out by experiments and earlier calculations [8–17].

3.3. Molecular orbitals

The molecular orbitals (MO) of the systems under investigation are examined in order to get insights to the high binding energy of ATP molecule. A summary of the nature of molecular orbitals of MTP systems with net charges −3, −2 and −1 is presented in Table 5 as obtained from MP2/

Table 5
Details of Molecular Orbitals and their energies of MTP at 6-31++G**

MO no.	Eigenvalues (in ev)					Atomic orbitals with significant contribution to the MOs
	MP2(−3)[a]	MP2(−2)	MP2(−1)	DFT(−1)	HF(−1)	
1–3	−79.72 to −79.70	−79.89 to −79.85	−80.03 to −80.02	−77.15 to −77.14	−80.02 to −80.00	1S of 'P'
4–13	−20.22 to −20.12	−20.36 to −20.26	−20.52 to −20.42	−19.09 to −19.01	−20.51 to −20.41	1S of 'O'
14	−10.94	−11.06	−11.21	−10.15	−11.41	1S of 'C'
15–17	−7.24 to −7.22	−7.40 to −7.37	−7.55 to −7.54	−6.59 to −6.58	−7.54 to −7.52	1S, 2S of 'P'
18–26	−5.14 to −5.12	−5.30 to −5.27	−5.45 to −5.44	−4.76 to −4.74	−5.44 to −5.42	2P*x*, 2P*y*, 2P*z* of 'P'
27	−1.04	−1.2	−1.37	−1	−1.38	4O(3S),3P(4S),5P(4S),2O(3S),4O(2S), 2O(2S),3P(3S),6O(3S),5P(3S),4O(4S), 6O(2S),7P(4S),6O(4S),4O(1S),2O(1S), 7P(3S)
28–36	−1.02 to −0.86	−1.16 to −1.01	−1.34 to −1.18	−0.99 to −0.85	−1.36 to −1.18	Mainly the high S orbitals of 'P' and 'O' (similar to 27th MO)
37	−0.59	−0.72	−0.88	−0.62	−0.88	MO of methyl group
38–40	−0.47 to −0.36	−0.62 to −0.53	−0.78 to −0.69	−0.56 to −0.45	−0.79 to −0.70	Mainly the high S and P orbitals of 'P' and 'O'
41–69	−0.32 to −0.23	−0.49 to −0.18	−0.64 to −0.35	−0.45 to −0.18	−0.66 to −0.34	The P orbitals of 'P' and 'O'
41	−0.32	−0.49	−0.64	−0.45	−0.66	4O(2P*x*),5P(3P*x*),6O(2P*x*),8O(2P*x*), 2O(2P*z*),3P(3P*x*),1C(2P*z*),8O(2P*z*), 2O(2P*y*),4O(2P*y*),4O(3P*x*),7P(3P*x*), 6O(3P*x*),18H(1S),8O(3P*x*),2O(3P*z*), 6O(2P*z*)
69 (HOMO)	−0.23	−0.18	−0.35	−0.18	−0.34	10O(2P*z*),9O(2P*y*),10O(3P*z*),9O(2P*x*), 9O(3P*y*),10O(2P*x*),9O(3P*x*),10O(3P*x*), 8O(2P*y*)
70 (LUMO)	0.28	0.22	0.11	0.08	0.12	15H(3S),1C(4S),3P(5S),1C(4P*z*), 5P(5S),2O(4S),16H(3S),17H(3S)

[a]The level of calculation; the numbers within the brackets represent the charge state.

Table 6
Details of Molecular Orbitals and their energies of MDP at 6-31++G**

MO no.	Eigenvalues (in ev)				Atomic orbitals with significant contribution to the MOs
	MP2(−2) [a]	MP2(−1)	DFT(−1)	HF(−1)	
1–2	−80.00 to −80.00	−80.00 to −79.97	−77.12 to −77.10	−79.98 to −79.94	1S of 'P'
3–9	−20.31 to −20.21	−20.48 to −20.38	−19.10 to −18.97	−20.47 to −20.36	1S of 'O'
10	−11.04	−11.19	−10.14	−11.18	1S of 'C'
11–12	−7.32 to −7.22	−7.51 to −7.48	−6.56 to −6.54	−7.50 to −7.46	1S, 2S of 'P'
13–18	−5.22 to −5.21	−5.41 to −5.38	−4.72 to −4.70	−5.40 to −5.36	2P*x*, 2P*y*, 2P*z* of 'P'
19	−1.12	−1.32	−0.97	−1.34	4O(3S),3P(4S),4O(2S),2O(3S),2O(2S),3P(3S),5P(4S), 4O(4S),5P(3S),6O(3S),6O(2S),4O(1S),2O(1S)
20–25	−1.10 to −0.95	−1.27 to −1.16	−0.93 to −0.81	−1.28 to −1.13	Mainly the high S orbitals of 'P' and 'O' (similar to 19th MO)
26	−0.69	−0.85	−0.6	−0.85	MO of methyl group
27–28	−0.55 to −0.45	−0.70 to −0.66	−0.50 to −0.46	−0.72 to −0.67	Mainly the high S and P orbitals of 'P' and 'O'
29–49	−0.40 to −0.12	−0.60 to −0.30	−0.41 to −0.14	−0.62 to −0.29	The P orbitals of 'P' and 'O'
29	−0.4	−0.6	−0.41	−0.62	6O(2P*x*),4O(2P*x*),1C(2P*y*),2O(2P*y*),6O(3P*x*), 14H(1S),6O(2P*y*),5P(3P*x*),4O(3P*x*),3P(3P*x*),11H(1S), 5P(3P*y*),2O(3P*y*),11H(2S),1C(3P*y*),6O(3P*y*)
49 (HOMO)	−0.12	−0.3	−0.14	−0.29	10O(2P*y*),9O(2P*y*),4O(2P*z*),7O(2P*x*),8O(2P*x*),9O(2P*z*), 10O(2P*z*),4O(3P*z*),7O(2P*z*),8O(2P*z*),10O(3P*y*), 9O(3P*y*),8O(2P*y*),7O(2Py),7O(3Px),8O(3P*x*),10O(2P*x*), 9O(2P*x*),9O(3P*z*),10O(3P*z*),7O(3P*z*),8O(3P*z*),8O(3P*y*), 7O(3P*y*),10O(3P*x*),9O(3P*x*)
50 (LUMO)	0.21	0.13	0.08	0.13	1C(4S),11H(3S),2O(4S),1C(4P*y*),13H(3S),12H(3S), 3P(5P*x*),5P(5S),4O(4P*x*),2O(4P*x*),3P(4S),5P(4S), 1C(3S),5P(5P*x*),1C(4P*x*),5P(4P*x*),3P(4P*y*), 1C(3P*x*),7O(4S),8O(4S),5P(5P*y*),13H(2S),12H(2S), 5P(4P*y*),11H(2S)

[a]The level of calculation; the numbers within the brackets represent the charge state.

6-31++G**. Similar results obtained for MTP(−1) at DFT/6-31++G** and HF/6-31++G** levels are also presented for comparison. Table 6 shows the molecular orbital compositions for MDP(−2) and MDP(−1) from MP2/6-31++G** and results for MDP(−1) at DFT/6-31++G** and HF/6-31++G** levels are presented for comparison.

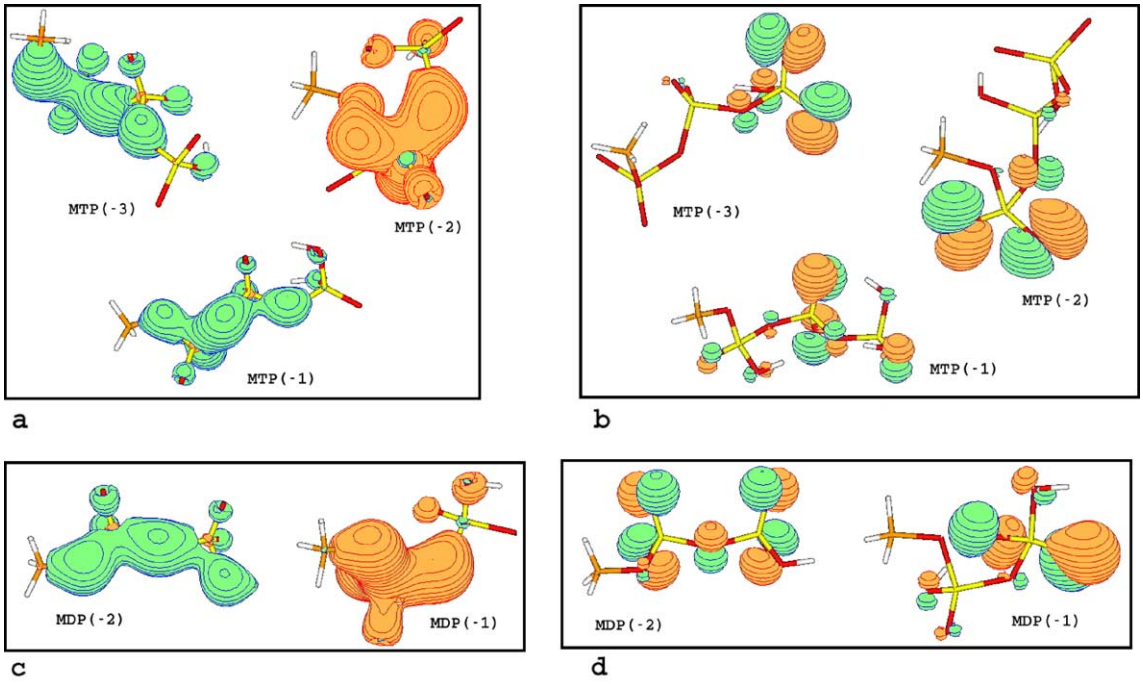

Fig. 3. (a) 27th and (b) 69th Molecular Orbitals of MTP(−3), MTP(−2) and MTP(−1) and (c) 19th and (d) 49th Molecular Orbitals of MDP(−2) and MDP(−1) at MP2/6-31++G**.

MTP(−3,−2,−1) systems consist of 138 electrons, which can be accommodated in 69 molecular orbitals. There is a remarkable consistency in the composition of MOs irrespective of the protonation state. The order of eigenvalues in all the protonated states corresponds to similar MOs, although they differ slightly in magnitude. The MOs from 1–26 are highly localized on specific atoms and the delocalization begins from the 27th MO. The 27th MO has significant contribution from the s-orbitals of higher principle quantum number of 'P' and 'O' atoms. A graphical representation of this MO for MTP(−3,−2,−1) at MP2/6-31++G** is given in Fig. 3a. The p-orbitals of 'P' and 'O' atoms begin to overlap at the 41st MO and a variety of atomic orbital combinations of these orbitals are made till the 69th MO, which is the highest occupied molecular orbital (HOMO, Fig. 3b). The energies of these MOs range from −0.638 ev to −0.176 ev at MP2/6-31++G** that depend on the protonation state. The MO configurations are very similar at all the levels of theory though the absolute energy values are different. It can be seen from Table 5 that the energies at DFT levels are lower than those at MP2 level. Forty three delocalized MOs (27th to 69th) with close spacing of energies as seen in MTP (irrespective of the protonation state) is indeed significant from the point of view of electron delocalization across the molecule. Similarly there are thirty one delocalized MOs (19th to 49th) in MDP (Table 6). It reduces to nineteen delocalized MOs in MMP. The 19th MO in MDP is highly delocalized as seen in Fig. 3c. Similarly, Fig. 3d shows the highest occupied molecular orbitals (HOMO) in MDP systems. From the above analysis, it seems that the hydrolysis of MTP→MDP+Pi and MDP→MMP+Pi disrupts twelve delocalized MOs. Thus, the source of high energy due to ATP hydrolysis in biological reactions probably arises due to such unusual nature of bonding involving a large number of delocalized MOs as seen in MTP. The process of hydrolysis itself is driven by environmental dependent factors such as the charge state, pH etc as discussed in section 3.2.

3.4. Frequency analysis

Vibrational frequency analysis can give insights to the changes that take place during a chemical or biological reaction. For instance, the GTP hydrolysis by GTPase has been investigated from Fourier transform infrared (FTIR) difference spectroscopy by monitoring the differences in the spectra of phosphate groups [19]. Also, IR spectroscopy and ab initio calculations have demonstrated that the phosphodiester groups of nucleic acids mediate the binding of extra cellular polymeric substances to mineral surfaces [18]. The assignments of the frequencies due to specific groups can be quantitatively made from ab initio frequency evaluation, which can aid in better understanding of experimental results [29,30]. The raw frequency values obtained from our studies at MP2/6-31++G** level are presented in this section. Although corrections are needed to obtain accurate frequencies [31], relative comparison of the raw values can give useful information on the differences between different species.

In the present study the predicted vibrational spectra have no imaginary frequencies (except for MDP(−2) [(t,t) conformation] which gives three imaginary frequencies) demonstrating that the optimized geometries are located at the minimum point of the potential surface. There are 48, 51 and 54 normal modes in total for MTP(−3), MTP(−2) and MTP(−1), respectively and 36 and 39 normal modes for MDP(−2) and MDP(−1), respectively. Plots of IR intensities vs. wave numbers for MTP and MDP are presented in Fig. 4. The high intensity modes and their corresponding frequencies (only for phosphate groups) are tabulated in Tables 7 and 8, respectively for MTP and MDP systems. From these tables one can observe that the strongest scattering mode of phosphate groups in MTP(−1) and MTP(−2) are (2859 cm^{-1}, 909 KM/Mole) and (2695 cm^{-1}, 1330 KM/Mole), respectively. These modes corre-

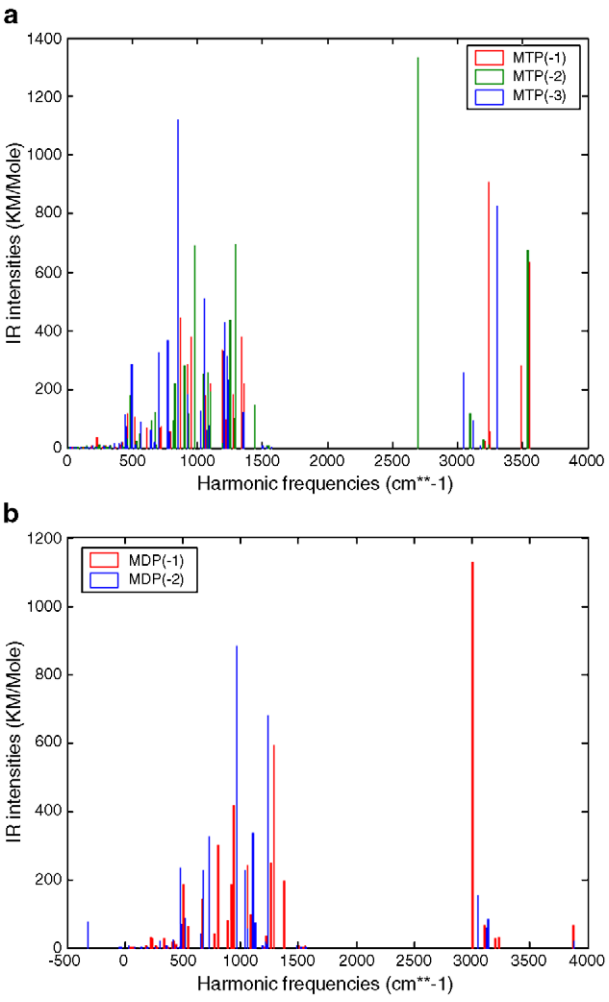

Fig. 4. IR spectra of (a) MTP and (b) MDP as obtained from MP2/6-31++G**.

Table 7
Calculated wave numbers (cm^{-1}), IR intensities (KM/Mole) and the vibrational modes of MTP at MP2/6-31++G** level

Sl No.	Mode of vibration[a]	MTP(−1)		MTP(−2)		MTP(−3)	
		Frequency	Intensity	Frequency	Intensity	Frequency	Intensity
1	O_8-H_{18} stretch	3548(54)	634	3538(51)	672	3303(48)	826
2	$O_{10}-H_{19}$ stretch	3488(53)	282				
3	$O_{14}-H_{20}$ stretch	2859(51)	909				
4	$O_{12}-H_{19}$ stretch			2695(47)	1330		
5	$P_7-O_8-H_{18}$ bend	122741)	235	1294(42)	692	1355(41)	120
6		1197(38)	334				
7	$P_7-O_{10}-H_{19}$ bend	1358(45)	221				
8	$P_3-O_{14}-H_{20}$ bend	1337(44)	337				
9		1251(42)	225				
10		828(30)	189				
11	$P_5-O_{12}-H_{19}$ bend			1443(43)	144		
12	P_7 group	934(34)	285	1210(38)	164	1200(36)	328
13		849(31)	542	1101(36)	189	1055(33)	511
14				1050(34)	250	856(30)	1122
15				829(29)	218	774(28)	367
16	P_5 group	1276(43)	182	1252(40)	434	1213(38)	427
17		1067(36)	178	981(33)	688	1029(32)	123
18		869(32)	444	936(32)	117	929(31)	182
19				925(31)	146	703(27)	327
20				904(30)	279		
21	P_3 group	956(35)	379	1283(41)	99		
22		924(33)	139	1082(35)	257		
23	All groups	520(23)	104	679(26)	121	498(21)	283
24		466(20)	117	485(21)	178	446(18)	114

[a]In modes 1–11, the H atoms are involved in hydrogen bonding (Fig. 2) and these modes were easier to identify from Molden[25]. In the other modes only the groups involved in the vibration could be identified.

spond to O–H bond stretching. However, in the case of MTP(−3) the strongest mode (856 cm^{-1}, 1122 KM/Mole) corresponds to the vibration of phosphate groups involving P_7 atom. In this case, the second strongest mode (3303 cm^{-1}, 826 KM/Mole) corresponds to O–H bond stretch.

Table 8
Calculated wave numbers (cm^{-1}), IR intensities (KM/Mole) and the vibrational modes of MDP at MP2/6-31++G** level

Sl No.	Mode of vibration[a]	MDP(−1)		MDP(−2)	
		Frequency	Intensity	Frequency	Intensity
1	O_6-H_{14} stretch	3871(39)	63		
2	$O_{10}-H_{15}$ stretch	3005(35)	1404		
3	$P_3-O_{10}-H_{15}$ bend	1377(31)	193		
4	$P_5-O_6-H_{14}$ bend			1107(24)	335
5	P_5 group	1289(30)	590	1040(22)	227
6		1086(25)	96		
7		1060(24)	241		
8	P_3 group	1261(29)	247	677(19)	228
9		1107(26)	181		
10		944(23)	416		
11		917(22)	185		
12		888(21)	79		
13	All groups	810(20)	301	1239(29)	677
14		673(18)	142	970(21)	881
15		510(16)	185	732(20)	323
16				480(15)	232

[a]In modes 1–4, the H atoms are involved in hydrogen bonding (Fig. 2) and these modes were easier to identify from Molden[25]. In the other modes only the groups involved in the vibration could be identified.

Similarly, the highest intensity mode of phosphate groups in MDP(−1) corresponds to O–H stretch as reported in Table 8. However, this is not true for MDP(−1). There are no O–H stretching frequencies in this case. The strongest scattering mode (970 cm^{-1}, 881 KM/Mole) here corresponds to overall motion of the molecule. From Tables 7 and 8 it is evident that the high frequency modes (>2800 cm^{-1}) are involved with OH bond stretching in MTP and MDP and these bonds are involved in hydrogen bond formation in these compounds. Similarly, the next higher frequencies (1000–1500 cm^{-1}) characterize the bending of P–O–H groups. There is a wide range of frequencies (400–1300 cm^{-1}) for different modes of vibrations involving phosphate groups. The actual values of these modes depend on factors such as the protonation state and the number of phosphate groups in the molecule. Thus, in principle, different species can be differentiated from such spectral values.

4. Conclusion

The tri- and diphosphate fragments of ATP molecule in different charge states have been investigated by ab initio quantum mechanical methods at the levels of HF, DFT and MP2. A consistent pattern of optimized geometries is seen from these different levels of calculations. The bond lengths and angles involving P and O atoms are depend-

ent on the number of phosphate groups and on the net charge of the molecule. Intramolecular hydrogen bonds play an important role in the overall geometries of these molecules.

Consistent energy patterns are obtained for the hydrolysis reactions of these pyrophosphate compounds by different levels of theory. The results confirm the earlier view that the electrostatic force is the driving force for the hydrolysis reaction.

Remarkable similarities are seen in the molecular orbital patterns irrespective of the level of calculation and the net charge of the molecule. A large number of molecular orbitals are highly delocalized through two or three phosphate units, which seem to explain the origin of high energy released during the hydrolysis of ATP. Possibly, the inherent nature of the pyrophosphates to acquire "high energy" character can be directly associated with the molecular orbital organization in the molecules.

The frequency analysis shows that the number of phosphate groups and the net charge in the molecule influences the frequencies corresponding to the vibration of the phosphate groups or the hydroxyl groups. These results may prove to be useful in understanding the biological events as followed through infrared spectroscopy.

Acknowledgements

We acknowledge the Computational Genomics Initiative at the Indian Institute of Science, funded by the Department of Biotechnology (DBT), India, for support. P. Hansia thanks the Council of Scientific and Industrial Research (CSIR), India for the award of fellowship.

Appendix A. Supplementary data

Supplementary data associated with this article can be found, in the online version, at doi:10.1016/j.bpc.2005.07.011.

References

[1] M. Baltscheffsky, P. Nyren, in: L. Ernster (Ed.), Bioenergetics, Elsvier, Amsterdam, 1984.
[2] M. Baltscheffsky, H. Baltscheffsky, in: L. Ernster (Ed.), Molecular Mechanism in Bioenergetics, Elsvier, Amsterdam, 1992.
[3] Y. Sugawara, N. Kamiya, H. Isawaki, T. Ito, Y. Satow, Humidity-controlled reversible structure transition of disodium adenosine 5′-triphosphate between dihydrate and trihydrate in a single crystal state, J. Am. Chem. Soc. 113 (1991) 5440–5445.
[4] F. Lipmann, Metabolic generation and utilization of phosphate bond energy, Adv. Enzymol. 1 (1941) 99–162.
[5] J.C. Sowden, H.O.L. Fischer, The chemistry and metabolism of the compounds of phosphorus, Ann. Rev. Biochem. 11 (1942) 203–216.
[6] H.M. Kalckar, The nature of energetic coupling in biological syntheses, Chem. Rev. 28 (1941) 71–178.
[7] P. Oesper, Sources of the high energy content in energy-rich phosphates, Arch. Biochem. Biophys. 27 (1950) 255–270.
[8] T.L. Hill, M.F. Morales, On "High Energy Phosphate Bonds" of biochemical interest, J. Am. Chem. Soc. 73 (1951) 1656–1660.
[9] K. Laki, M. Seel, J. Ladik, Conformation of triphosphate and lysine–triphosphate–arginine complex, J. Theor. Biol. 67 (1977) 489–498.
[10] W. Saenger, B.S. Reddy, K. Mühlegger, G. Weimann, X-ray study of the lithium complex of NAD, Nature 267 (1977) 225–229.
[11] D.M. Hayes, G.L. Kenyon, P.A. Kollman, Theoretical calculations of the hydrolysis energies of some "High-Energy" molecules: 2. A survey of some biologically important hydrolytic reactions, J. Am. Chem. Soc. 100 (1978) 4331–4340.
[12] M. O'keeffe, B. Domenges, G.V. Gibbs, Ab initio molecular orbital calculations on phosphates: comparison with silicates, J. Phys. Chem. 89 (1985) 2304–2309.
[13] C.S. Ewig, J.R. Van Wazer, Ab initio structures of phosphorus acids and esters. 3. The P–O–P bridged compounds $H_4P_2O_{2n-1}$ for $n=1$ to 4, J. Am. Chem. Soc. 110 (1988) 79–86.
[14] H. Saint-Martin, I. Ortega-Blake, A. Leś, L. Adamowicz, Ab initio calculations of the pyrophosphate hydrolysis reaction, Biochim. Biophys. Acta. 1080 (1991) 205–214.
[15] B. Ma, C. Meredith, H.F. Schaefer III, Pyrophosphate structures and reactions: evaluation of electrostatic effects on the pyrophosphates with and without alkali cations, J. Phys. Chem. 98 (1994) 8216–8223.
[16] M.E. Colvin, E. Evleth, Y. Akacem, Quantum chemical studies of pyrophosphate hydrolysis, J. Am. Chem. Soc. 117 (1995) 4357–4362.
[17] M. Hwang, P. Chu, J. Chen, I. Chao, Conformational analysis of three pyrophosphate model species: diphosphate, methyl diphosphate and triphosphate, J. Comput. Chem. 20 (1999) 1702–1715.
[18] C. Allin, M.R. Ahmadian, A. Wittinghofer, K. Gerwert, Monitoring the GAP analyzed H-Ras GTPase reaction at atomic resolution in real time, Proc. Natl. Acad. Sci. U. S. A. 98 (2001) 7754–7759.
[19] A. Omoike, J. Chorover, K.D. Kwon, J.D. Kubicki, Adhesion of bacterial exopolymers to α-FeOOH: inner-sphere complexation of phosphodiester groups, Langmuir 20 (2004) 11108–11114.
[20] P.C. Hariharan, J.A. Pople, The influence of polarization functions on molecular orbital hydrogenation energies, Theor. Chim. Acta 28 (1973) 213–222.
[21] G.A. Petersson, A. Bennett, T.G. Tensfeldt, M.A. Al-Laham, W.A. Shirley, J. Mantzaris, A complete basis set model chemistry: I. The total energies of closed-shell atoms and hydrides of the first-row elements, J. Chem. Phys. 89 (1988) 2193–2218.
[22] Gaussian 03, Revision C.02, M.J. Frisch, G.W. Trucks, H.B. Schlegel, G.E. Scuseria, M.A. Robb, J.R. Cheeseman, J.A. Montgomery Jr., T. Vreven, K.N. Kudin, J.C. Burant, J.M. Millam, S.S. Iyengar, J. Tomasi, V. Barone, B. Mennucci, M. Cossi, G. Scalmani, N. Rega, G. Petersson, H. Nakatsuji, M. Hada, M. Ehara, K. Toyota, R. Fukuda, J. Hasegawa, M. Ishida, T. Nakajima, Y. Honda, O. Kitao, H. Nakai, M. Klene, X. Li, J.E. Knox, H.P. Hratchian, J.B. Cross, V. Bakken, C. Adamo, J. Jaramillo, R. Gomperts, R.E. Stratmann, O. Yazyev, A.J. Austin, R. Cammi, C. Pomelli, J.W. Ochterski, P.Y. Ayala, K. Morokuma, G.A. Voth, P. Salvador, J.J. Dannenberg, V.G. Zakrzewski, S. Dapprich, A.D. Daniels, M.C. Strain, O. Farkas, D.K. Malick, A.D. Rabuck, K. Raghavachari, J.B. Foresman, J.V. Ortiz, Q. Cui, A.G. Baboul, S. Clifford, J. Cioslowski, B.B. Stefanov, G. Liu, A. Liashenko, P. Piskorz, I. Komaromi, R.L. Martin, D.J. Fox, T. Keith, M.A. Al-Laham, C.Y. Peng, A. Nanayakkara, M. Challacombe, P.M.W. Gill, B. Johnson, W. Chen, M.W. Wong, C. Gonzalez, J.A. Pople, Gaussian, Inc., Wallingford CT, 2004.
[23] A.D. Becke, Density functional thermochemistry: III. The role of exact exchange, J. Chem. Phys. 98 (1993) 5648–5652.
[24] M. Head-Gordon, J.A. Pople, M.J. Frisch, MP2 energy evaluation by direct methods, Chem. Phys. Lett. 153 (1988) 503–506.
[25] G. Schaftenaar, J.H. Noordik, Molden: a pre- and post-processing program for molecular and electronic structures, J. Comput. Aided. Mol. Des. 14 (2000) 123–134.

[26] G.A. Jaffrey, J.A. Pople, J.S. Binkley, S. Vishveshwara, Application of ab initio molecular orbital calculations to the structural moieties of carbohydrates. 3, J. Am. Chem. Soc. 100 (1978) 373–379.
[27] D.G. Gorenstein, Conformation and dynamics of DNA and protein–DNA complexes by 31P NMR, Chem. Rev. 94 (1994) 1315–1338.
[28] D.G. Gorenstein, J.B. Findlay, B.A. Luxon, D. Kar, Stereoelectronic control in carbon–oxygen and phosphorus–oxygen bond breaking processes. Ab initio calculations and speculations on the mechanism of action of ribonuclease A, staphylococcal nuclease, and lysozyme, J. Am. Chem. Soc. 99 (1977) 3473–3479.
[29] W. Förner, H.M. Badawi, Ab initio calculations of vibrational frequencies, potential functions of internal rotations and vibrational infrared and Raman spectra for 3,3,3-trifluoropropanal, J. Mol. Model 6 (2000) 99–111.
[30] W. Li, Q. Wu, Q.Y. Ye, M. Luo, D. Shi, J. Hu, Density functional and ab initio studies of the molecular structure and vibrational spectra of novel O,O'-diethyl-*N*-(alpha-aryloxyacetyl)thiophosphoryl hydrazine herbicides, J. Raman Spectrosc. 34 (2003) 892–901.
[31] A.P. Scott, L. Radom, Harmonic vibrational frequencies: an evaluation of Hartree–Fock, Moller–Plesset, quadratic configuration interaction, density functional theory, and semiempirical scale factors, J. Phys. Chem. 100 (1996) 16502–16513.